INTRA DIURNAL AND SEASONAL VARIABILITY OF SOIL TEMPERATURE, HEAT FLUX, SOIL MOISTURE CONTENT, AND THERMAL PROPERTIES UNDER FOREST AND PASTURE IN RONDONIA

R. C. S. Alvalá[1]; R. Gielow[1]; H. R. da Rocha[2]; H. C. Freitas[2]; J. M. Lopes[2]; A. O. Manzi[1]; C. von Randow[1]; M. A. F. S. Dias[2]; O. M. R. Cabral[3]; M. J. Waterloo[4]

(1) Instituto Nacional de Pesquisas Espaciais, Brazil

(2) Universidade de São Paulo, Brazil

(3) CNPMA-EMBRAPA, Brazil

(4) Alterra, The Netherlands

To be submitted

Journal of Geophysical Research - Atmospheres

Abstract

Soil temperatures depend on the soil heat flux, an important parameter in meteorological and in plant growth-energy balance models. Thus, they were measured, together with soil moisture contents, within the LBA program at forest (Reserva Jaru) and pasture (Fazenda Nossa Senhora) sites in Rondônia, Brazilian Amazonia, during wet (February) and dry (August) periods of 1999. The wet period showed maxima of the heat flux into the soil around five to six times smaller at the forest than at the pasture, except for some spikes which are related to stronger solar forcing, such as those due to sunspecks in the forest. This pattern remained during the dry period, but with doubled maximum values. Also, the soil heat flux and the soil temperatures responded very significantly to the passage of cold fronts in both periods at both sites. Temperature profiles measured in the 10 to 40 cm soil layer showed daily averages and ranges smaller at the forest than at the pasture. The daily average of the soil moisture content in the same layer, during the wet season, increased with depth at both sites, with consistently lower values at the forest; however, their ranges were smaller at the pasture, except for the 40 cm depth. During the dry period, these ranges were much higher at the pasture, but with nearer average values. Finally, the computed daily apparent soil thermal diffusivities, volumetric heat contents and thermal conductivities are presented, with the first ones crossed with the measured soil moisture content.

1. Introduction

Heat and moisture exchanges between the ground surface and the atmosphere are frequently dominant driving mechanisms for mesoscale circulations. These surface processes are included in weather forecast model physics by specifying different lower boundary conditions, which depend on the soil and surface characteristics, thus presenting spatial variation. Over land, significant diurnal changes of temperature and moisture balance near the interface with the atmosphere also occur (Smith et al, 1994; Smirnova et al., 1997). In particular, the prediction of the ground surface temperature and moisture content is critical to obtain successful forecasts of the above mentioned exchanges.

Coupled models of heat and moisture transport in bare soils (Novak and Black, 1985; Passerat de Silans et al, 1989) or in vegetated soils (Braud et al., 1994; Smirnova et al, 1997) require information about soil thermal properties, such as thermal conductivity, thermal diffusivity, and volumetric heat capacity, which are used to determine temperature profiles and heat flux in the soil. These properties (de Vries, 1966) are dependent on soil moisture content, soil composition and structure, and vegetation cover (shading, root influence on soil moisture content). Notwithstanding, these data, especially as a function of water content, are currently not readily available, despite their increasing demand, due to more detailed requirements of the transport models.

The soil thermal properties, due to their dependency on the soil moisture content, vary both in space and in time causing two types of heterogeneity (Verhoef et al., 1996). A meso-scale heterogeneity that can be induced by spatially variable rainfall which influences these properties

(and thus the soil heat flux and temperature) through changes in soil moisture content on a scale of several kilometers. Second, a heterogeneity on the micro-scale, which depends on the conditions of the surface, that is, bare or covered with vegetation. The cover may be dense or present different degrees of sparseness. This will influence the underlying soil by shading it homogeneously or not, with influence on the soil moisture, and thus the soil thermal properties. Besides these spatial variations, large temporal variations occur if heavy rainfall is alternated by dry periods.

Also, all of the physical, chemical, and the biological processes which occur in the soil are influenced by the soil temperature and moisture content, and their gradients. Biological processes such as the uptake of nutrients and water by roots, the decomposition of organic matter by microbes and the germination of seeds are strongly affected by them. Rates of some of these processes more than double for each 10 C increase in temperature. In some cases, growth of above-ground plant parts is more closely correlated with soil temperature than with air temperature. Physical processes, such as water movement and soil drying can also be strongly influenced by temperature (Campbell, 1985).

This paper describes the intra diurnal and seasonal variability of soil temperature, heat flux and moisture content during wet and dry periods, as well as some aspects of the dry-wet transition period, all measured in 1999 at forest (Reserva Jaru) and pasture (Fazenda Nossa Senhora) sites in Rondonia, Brazilian Amazonia, within the WETAM/LBA project and its subsequent field observations. Also, corresponding computed values of thermal properties of the soil are presented.

2. Sites Descriptions, Soil Characteristics and Field Measurements

The data were collected at the pasture site on the Nossa Senhora farm - NS (10°45' S, 62°22' W) and in the forest of the Reserva Biológica do Jaru - RJ (10°46' S, 61°56' W), both located near Ji-Paraná in the state of Rondônia, in the western part of Brazil. The Nossa Senhora farm is a cattle ranch 220 m above sea level about 50 km north east of Ji-Paraná, which was deforested about twenty years ago. This farm is situated in a strip of cleared land about 4 km wide and several tens of kilometers long, in the center of an area of about 50 km in radius, which has been largely cleared and covered with grass [*Brachiaria brizantha* (A. Rich.) *Stafp*]. Reserva Jaru is a forest reserve owned by the Brazilian Environmental Protection Agency (Instituto Brasileiro de Meio Ambiente e Recursos Renováveis, IBAMA), and is located about 80 km north of Ji-Paraná at 120 m above sea level. Details of the vegetation and soil at both sites are given by *McWilliam et al*. (1996) and by *Hodnett et al.* (1996), respectively.

The main observation periods considered in the present study, (i) February and (ii) August 1999, represent the end of both the rainy and the dry seasons, while (iii) September 1999 constitutes the transition from dry to rainy season in the region considered.

The dry bulk densities (ρ) and porosities of the soil at both sites, which contain more than 70% of sand, were determined at the depths of 0.025, 0.10, 0.20 and 0.40 m, as shown in Table 1.

Two profiles of soil temperatures in both pasture and forest were sampled with Campbell Scientific thermistors (Logan, UT, USA), with determination of 10 minutes averages. At Fazenda

Nossa Senhora the soil temperatures were measured at three depths: 0.10, 0.20 and 0.40 m, while at Rebio Jaru one profile was measured at the same three depths, and the second at two depths: 0.10 and 0.20 m.

The soil heat flux was measured at both sites at 0.02 m with Campbell heat flux plates. The incident and reflected solar radiations were measured with Kipp and Zonen solarimeters (Delft, the Netherlands), the net radiation was obtained with REBS net radiometers (Seattle, WA, USA), and the air temperature and relative humidity were measured with an HMP45C-L150 thermo-hygrometer (Vaisala, Finland). These instruments were installed on aluminum towers, at the heights of 6.72 m in the pasture site and of 58.35 m in the forest site, respectively. The rainfall was measured at both sites with 0.2 mm resolution tipping bucket raingauges from Didcot (Abingdon, UK).

The soil moisture content (θ) was sampled by frequency domain reflectometry - FDR sensors (FDR Campbell Systems CS615 sensors, Logan, UT, USA) at three depths: 0.10, 0.20 and 0.40 m, with two profiles at the pasture and one at the forest, with a data acquisition rate of 10 min averages. The calibration curves for the FDRs were adjusted through laboratory tests using undisturbed soil samples from both sites, resulting the following expressions:

Rebio Jaru $$\theta = 0.379t^2 + 0.154t - 0.343 \quad (1)$$

Fazenda Nossa Senhora $$\theta = 1.044t^2 - 1.035t + 0.183 \quad (2)$$

where t is the response time in ms.

The resulting soil moisture contents were also compared with corresponding gravimetric determinations in soil samples collected in the neighborhood of the FDRs, as presented in Table 2.

3. Soil Thermal Properties

Temperature profiles in the soil may be obtained through the integration of the heat conduction equation,

$$C\frac{\partial T}{\partial t}=\frac{\partial}{\partial z}\left(\lambda\frac{\partial T}{\partial z}\right) \tag{3}$$

where T is temperature in °C, t is time in s, z the depth in m, C the volumetric heat capacity of the soil (J m^{-3} K^{-1}), and λ is its apparent thermal conductivity in W m^{-1} K^{-1}. Also,

$$C = \rho\, C_b \tag{4}$$

$$\lambda = C\,\alpha \tag{5}$$

where α is the apparent thermal diffusivity in m^2 s^{-1}, ρ is the bulk density of the soil in kg m^{-3} and C_b is the bulk specific heat in J Kg^{-1} K^{-1}. However, these parameters vary with the composition, texture and moisture content of the soil. For a soil with a negligible organic fraction, the

volumetric heat capacity, as shown by Campbell (1985) and following de Vries (1966), may be obtained from

$$C = \frac{\rho}{\rho_m} C_m \ + \theta \, C_w \tag{6}$$

where C_m and C_w are the specific heats of the mineral constituents of the soil and of water respectively, ρ_m is the density of the mineral fraction and θ ($m^3\ m^{-3}$) is the volumetric moisture content of the soil. In this work, the mineral constituents are considered as being quartz. Thus, $\rho_m = 2650$ kg m^{-3}, $C_m = 2.13$ MJ m^{-3} K^{-1} and $C_w = 4.18$ MJ m^{-3} K^{-1} .

The apparent thermal diffusivity, which is considered to be constant for a uniform soil, can be determined by several methods using measurements of transient soil temperature. These methods are based on either analytical or numerical solution of the equation of heat conduction, and six of them were evaluated by Horton et al. (1983). However, as actual soils are vertically non-uniform, with varying composition, texture and moisture content, more elaborate methods should be used (Lettau, 1953; van Wijk and Derksen, 1966, Nassar and Horton, 1989).

Alternatively, the non-uniform soil may be divided into layers, each considered to be of uniform composition and structure, in which α and C are assumed constant. So, Equation 3 becomes

$$\frac{\partial T}{\partial t} = \alpha_j \left(\frac{\partial^2 T}{\partial z^2} \right) \tag{7}$$

where $\alpha_j = (\lambda / C)_j$, is the apparent thermal diffusivity of layer j, limited by z_{j-1} and z_{j+1}, j = 1, 2, ...m, the number of layers, not necessarily of equal thickness (Alvalá et al., 1996). It should be noted that in this case there is no explicit dependence of the apparent thermal diffusivity on the soil moisture content, if the temperature series are known.

The apparent thermal diffusivity may be determined by the use of measured soil temperatures substituted into expressions obtained from analytical solutions of Equation 7. This is the case for the methods shown by Horton et al. (1983) and referred as the "periodic" methods; they require measured temperature time series in two soil levels, and no initial vertical profile. Otherwise, numerical solutions of Equation 7, for measured initial plus upper and lower boundary conditions, may also be obtained with a succession of assumed values of α, followed by the comparison of the computed temperature series with the measured ones, to find the value of α which minimizes the root mean squared (RMS) differences between the measured and computed series inside the soil layer considered. This method requires measured temporal temperature series in at least three soil levels; however, it allows for any initial and boundary conditions, as opposed to the periodic methods, which presuppose sinusoidal (or Fourier series) boundary conditions. Finally, an upper limit for the apparent thermal diffusivity, as function of the soil moisture content, is obtained through the linear superposition of the thermal diffusivities of the mineral, water and air volumetric fractions of the soil layer under study, that is

$$\alpha_j = \frac{\rho}{\rho_m}\alpha_m + \theta\alpha_w + (1 - \frac{\rho}{\rho_m} - \theta)\alpha_{air} \qquad (8)$$

where the mineral fractions is considered as quartz and the small organic contribution is neglected. The actual apparent soil thermal diffusivity is smaller, because the heat transport inside the soil is not uniform, presenting internal resistances due to its pores and their air-water content.

In this work, Equation 7 was put in the form of non-equally spaced finite differences by means of a second order weighted scheme (Ralston and Wilf, 1964; Campbell, 1985). The apparent thermal diffusivity was then obtained by successive iterations using the RMS minimizing procedure shown by Alvalá et al. (1996), for 24 hours LST periods. The initial estimate of the apparent thermal diffusivity was determined by the amplitude periodic method; it was usually higher than the value which minimized the above mentioned RMS. Finally, the apparent soil heat conductivity was computed through Equation 5.

4. Results

The incident solar energy flux at the ground surface ($K\downarrow$) is the primary source for all other components of the radiation balance, while the net radiation (R_n) is partitioned into sensible and latent heats, soil heat flux (G), energy storage in the above ground biomass and liquid water cover, plus other minor terms. These variables affect both the soil and the air temperature and moisture content profiles. Thus, to characterize the wet February and dry August periods, the monthly statistics of measured daily accumulated energy fluxes at the forest and pasture sites

studied are shown on Tables 5 and 6. During the wet period, at both sites, the average daily accumulated K↓, which is inversely proportional to the density of the cloud cover, was smaller than during the dry period, indicating a denser cloud cover during the wet period. On the other hand, during the wet period, the daylight cloud cover was on the average heavier and with more variance at the forest, showed by an average daily accumulated K↓ equal to 16.8 ± 4.75 MJ m^{-2}, versus 17.37 ± 3.71 MJ m^{-2} at the pasture, a situation that was reversed during the dry period, with 18.84 ± 2.06 MJ m^{-2} versus 17.83 ± 3.71 MJ m^{-2}. For the average daily accumulated R_n, the values were 12.63 ± 3.53 MJ m^{-2} at forest and 11.27 ± 2.42 MJ m^{-2} at pasture during the wet period, followed by 11.01 ± 1.67 MJ m^{-2} and 7.74 ± 0.97 MJ m^{-2}, respectively, during the dry period, that is, a pattern identical to the one for K↓, with the exception of the smaller variance at the pasture during the dry period. The average daily accumulated R_n / K↓ was higher during the wet period at both sites, equaling 0.71 at the forest and 0.65 at the pasture, versus respectively 0.58 and 0.44 during the dry period, with values during the same period always higher at the forest. The daily accumulated values of G (AG), with maxima (daily heat accumulation in the soil causing its temperature to rise) of up to 2.6% of the daily accumulated R_n at the forest and 18.2 % at the pasture, and the respective minima (daily heat depletion in the soil) of up to 4.9 % and 11.1 %, respectively, show the importance of the soil heat flux. The lower values at the forest are consequences of a greater energy storage in its canopy, despite its consistently lower albedo, that is, less solar energy reflection. This also causes a consistently greater variance of the monthly average AG at the pasture, and consequently, greater daily soil temperature ranges, which influence the soil moisture content, that is, its evaporation process.

Next, the detailed results concerning the soil temperature, heat flux, moisture content, and thermal properties are presented.

4.1 Soil Temperature and Heat Flux

During the wet season month of February, the soil temperature at the depth of 10 cm at the forest (Figure 1c) presented an overall 10 minutes sampled average of 24.78 C, an absolute maximum of 25.85 C and an absolute minimum of 24.04 C (Table 3), while the corresponding values at the pasture (Figure 2c) were 26.59 C, 31.09 C and 23.67 C (Table 3). Thus, except for the 10 cm minimum, the values at the forest were smaller than at the pasture, including the range between corresponding maxima and minima. Without the exception mentioned, this was also the behavior at the 20 and 40 cm depths, with smaller ranges between the extrema at both sites, as evidenced by their respective monthly standard deviations (Figures 1c and 2c, Table 3). Non-evenness in the daily cycling of the signals is due to the passage of clouds, with or without rainfall. During the dry season month of August (Figures 3c and 4c, Table 4), the behavior was similar but with a smoother cycling of the signals, except during the passage of a strong cold front, which is described below.

The soil heat flux during February, at both sites, presented strong influence of the passage of clouds and rainfall, mixed with some direct sunshine, which caused sunflecks in the forest. So, the passage of clouds brought non-smoothness to this signal, while the sunflecks caused positive spikes and rainfall negative ones, as can be seen on Figures 1d and 2d. The 10 minutes averages sampled soil heat flux range at the forest, except for occasional spikes, was from –16.3 to 21.0 W m^{-2}, while at the pasture it ranged from –32.0 to 167.1 W m^{-2}. The spikes associated with

sunflecks at the forest reach 177.1 W m^{-2}, while rain episodes cause spikes of up to –58.4 W m^{-2} at the forest, and -147.7 W m^{-2} at the pasture. The last ones are clear signatures of concentrated rainfalls (Figures 1f and 2f). They may be used to verify their occurrence in the absence of actual measurements, as eventually was the case during the experiment, such as on DOY 56 at the pasture, also evidenced by the soil moisture content change shown on Figure 2e. Also, it is interesting to note that on DOY 38 a squall line, originated over the Atlantic Ocean and combined with a cold front, brought rainfalls of 24.40 mm at the forest and 28.2 mm at the pasture. From DOY 37 to 38 the maximum air temperature decreased from 30.4 C to 24.2 C at the forest (Figure 1a), and from 31.39 C to 29.48 C at the pasture (Figure 1b). The corresponding decreases of the maximum soil temperatures at the forest occurred at the same time; however, at the pasture they were delayed by one day. Notwithstanding, the soil heat flux presented a spike of –147.17 W m^{-2} at the pasture, and none at the forest. On the other hand, the total rainfalls of 48.3 mm at the forest and 42.99 mm at the pasture, which occurred on DOYs 48 and 49, caused a strong decrease of the maxima of the soil temperatures, but not on the maximum air temperatures; also, the soil heat flux presented spikes of -58.36 W m^{-2} at the forest and of –59.35 W m^{-2} at the pasture.

During the dry month of August, at both sites (Figures 3 and 4), the soil temperature and heat flux signals were smoother, but showing decreases in the extrema associated with the cold fronts that reached the region. A mild event occurred on DOY 220, with small temperature decreases and no rain associated. However, after sunset on DOY 225, a strong cold front reached the region, caused by a cold mass that affected most of Brazil (INPE, 1999). Its main measured temperature characteristics are presented on Figure 5. There was no rain at the forest, but at the

pasture occurred a 11.54 mm rainfall, with a -123.7 W m^{-2} soil heat flux spike. Concerning cold fronts, it should be noted that outside the periods presented above, on DOYs 187 (July 6), 262 (September 19) and 276 (October 3) milder ones reached the region. Also, still in August, on DOY 241 there was a 50 mm rainfall at the pasture, with a soil heat flux spike of -127.57 W m^{-2}, while on DOY 242 occurred a 12.59 mm of rainfall at the forest, with a – 44.35 W m^{-2} spike caused by the first 0.16 mm of this precipitation, which was the first one at this site after a 60 days long dry-spell.

4.2 Soil Moisture Content

The soil moisture content (SMC), at the depths of 10, 20 and 40 cm, increased after a rainfall event and immediately started to decrease until the next rain, indicating that water in these sandy soils rapidly drains toward deeper layers during rainfall events, as it is shown on Figures 1e and 2e for both sites during the wet month of February. Notice that the SMC normally increases with depth, except immediately after most rainfall events at the forest, such as those of DOYs 38, 40, 45, 48 and thereafter, when the more superficial layer was wetter. However, at the pasture this inversion seldom occurred. The rates of drying were higher nearer to the surface at both sites. Also, on non rainy days, these rates were higher during the daylight hours and decreased at night, as may be seen after DOY 38 at the pasture (Figure 2e); this behavior, which is less intense at the forest, reflects the presence or not of sunlight and its intensity. The drying gradients are lower at the forest than at the pasture site, which can be better seen during August and September at both sites, such after the rainfalls of 12.6 mm on DOY 242 (August 30) at the forest and 50.36 mm on DOY 240 at the pasture (Figures 3e, 4e, 6 and 7).

The maximum soil moisture content at the forest was 0.39 m^3 m^{-3} at the depth of 10 cm, and 0.30 m^3 m^{-3} at 40 cm, both on DOY 78 (March 19). At the pasture, these maxima were respectively 0.34 and 0.40 m^3 m^{-3}, both on DOY 49 (February 18). In each site, after the days cited, the SMC diminished, with increases caused by eventual rainfalls.

So, at the forest, after 34.39 mm of rainfall between DOYs 123 (May 3) and 170 (June 19) and a precipitation of 28.80 mm from DOYs 171 to 183 (June 20 to July 2), a dry-spell of 37 days occurred up to DOY 243 (August 31), when a 12.6 mm rainfall occurred. It was then followed by a rain of 30 mm on DOY 259 (September 16). This last day may be considered the beginning of the new wet season at the forest, with initially sparse but intense rains above 30 mm each – see Figure 6. The minima of SMC at the forest were 0.06 m^3 m^{-3} at 10 cm and 0.09 m^3 m^{-3} at 40 cm, both on DOY 242 (August 30).

At the pasture, after rainfalls totaling 4.18 mm between DOYs 134 (May 14) and 173 (June 23), followed a rainfall of 44.97 mm on DOY 174 (June 24) plus a total of 13.13 mm precipitation from DOYs 175 to 184 (June 25 to July 3); then, it did not rain until DOY 254 (September 11), except for the DOY 225 (August 13, with 12.4 mm and a small increase of the SMC only at the depth of 10 cm) and the DOY 240 (August 28, with 50 mm and a steep increase of the SMC at all depths). Thereafter, actually on DOY 263 (September 20), started the new rainy season, with immediate increase of the SMC at the pasture (Figure 7). The minima of SMC were 0.04 m^3 m^{-3} at 10 cm and 0.09 m^3 m^{-3} at 40 cm, both on DOY 242.

During the transition from dry to wet season at the pasture (Figure 7), when the SMC at 40 cm increased from 0.13 m^3 m^{-3} on DOY 262 to 0.28 m^3 m^{-3} on DOY 269, the soil was wetter at the 10 and 20 cm depths; thereafter, the normal pattern of increasing wetness with depth was re-established. At the forest site, there was no inversion of patterns at the beginning of the new wet season, when on DOY 258 the SMC at 40 cm started to increase from 0.1 m^3 m^{-3} to 0.23 m^3 m^{-3} on DOY 262, a response to a 73.01 mm of rainfall. The SMC was lower at the forest than at the pasture site during the wet season, while the opposite occurred during the dry months. Finally, for both sites, as shown on Figure 8, a unique linear relation between the daily averages of the SMC and the accumulated moisture content in the 10-40 cm soil layer was determined.

4.3 Soil Thermal Properties

The computed apparent daily average volumetric soil heat capacities - C, which are linearly dependent on the SMC, are presented on Figures 9 to 12 for both periods and sites, jointly with the daily rainfalls, the average SMC for the 10-40 cm soil layer, the apparent soil thermal diffusivities and conductivities. The C values are lower at the forest than at the pasture site during the wet February period, a situation that is reversed during the dry August period, as a consequence of the moisture condition of the soil. Their monthly statistics are shown on Table 7, with averages for the wet period equal to 2.11 ± 0.10 MJ m^{-3} K^{-1} at the forest and 1.34 ± 0.37 MJ m^{-3} K^{-1} at the pasture. For the dry period these values were, respectively, 1.60 ± 0.03 MJ m^{-3} K^{-1} and 1.64 ± 0.14 MJ m^{-3} K^{-1}.

The computed apparent daily soil thermal diffusivities (α) and the corresponding bias and RMS deviations between the measured and computed soil temperatures, for both sites and periods, are shown on Figures 9 to 12 and Table 7; the monthly statistics for these bias and RMS are presented on Table 8. Their monthly averages for the wet period were $1.08 \times 10^{-6} \pm 0.44$ m^2 s^{-1} for the forest and $1.34 \times 10^{-6} \pm 0.37$ m^2 s^{-1} for the pasture, while for the dry period these values were, respectively, $0.55 \times 10^{-6} \pm 0.33$ m^2 s^{-1} and $1.16 \times 10^{-6} \pm 0.14$ m^2 s^{-1}. The diffusivities have a behavior similar to the one shown by the apparent daily volumetric soil heat capacities, which is proportional to the SMC. Notwithstanding, a clear dependency on SMC was not found, despite that each value was iteratively obtained (best fit) through the RMS minimization between measured and numerically computed temperatures. This is shown on Figure 13, with data from both sites, for non-rainy days, to avoid steep temporal SMC gradients during the days considered. Also, the best fits of the diffusivities, as shown by its bias and RMS on Figures 9 to 12 and Table 8, are variable. Their daily RMS values for the temperature adjustments vary between 0.02 and 0.40 C, and their bias from -0.34 and 0.37 C, for the sites and the dry and wet periods considered. The quality of the adjustment depended on the site and the period, as well the particular daily situation, such as clear or cloudy, with or without rain, as well as the presence or not of a cold front. Considering monthly statistics (Figure 8), except for the overestimation during the dry period at the forest, the values of α computed caused a relatively small underestimation of the temperatures at the 20 cm depth; Figure 14 shows some typical examples of these adjustments. On the other hand, all results obtained for the apparent soil thermal diffusivities, as expected, are lower than the values predicted by Equation 8, which increase linearly from 2.35×10^{-6} m^2 s^{-1} at SMC equal to 0.05 m^3 m^{-3} up to 2.40×10^{-6} m^2 s^{-1} at SMC equal to 0.40 m^3 m^{-3}. As mentioned, this is caused by the fact that this expression

presupposes a linear superposition of soil and water heat transport effects, while actually the system is not uniform, with internal heat transport resistances due to the pores of he soil and their air-water content.

The computed apparent daily soil heat conductivities (λ), obtained through Equation 5, during the wet season were equal to 2.28 ± 0.98 W m^{-1} K^{-1} at the forest and 3.20 ± 0.90 W m^{-1} K^{-1} at the pasture, while during the dry season they were equal to, respectively, 0.85 ± 0.54 W m^{-1} K^{-1} and 1.91 ± 0.33 W m^{-1} K^{-1}. The decline in λ between wet and dry periods corresponded to a decrease of 0.122 m^3 m^{-3} and 0.182 m^3 m^{-3} in soil moisture content for the 10-40 cm soil layer at forest and pasture, respectively.

5. Conclusions

The wet period was characterized by dense cloud covers at both sites, which were heavier and more variable along the daylight hours at the forest, as evidenced by the average daily accumulated incident solar radiation. During the dry period, with less dense cloud covers, this pattern was reversed, with lighter and less variable cloud covers at the forest. The average daily accumulated net radiation showed a pattern similar to the one of the average daily accumulated solar radiation, except for a smaller variance at the pasture during the dry period. The ratio between them was higher at both sites during the wet period than at the dry period, with greater values at the forest during a given period. The soil heat flux, presented daily accumulated values reaching maxima (which cause soil temperature rises) of up to 2.6% of the daily accumulated net

radiation at the forest, and up to 18.2% at the pasture, while the respective minima (which cause soil heat depletion) during wet period were respectively 9.7% and 41.2%. These extrema, due to smaller vegetation cover are greater at the pasture, determine the soil temperature ranges, and thus influence the soil moisture content.

During the wet period, the soil temperatures and their ranges at the depths of 10, 20 and 40 cm , except for a 10 cm minimum, were smaller at the forest, with non-evenness in their daily cycle due to the passage of clouds, with or without rainfall. The soil heat flux presented strong influences of the passage of clouds and rainfalls, intermixed with direct sunshine, with consequent non-smoothness of the signal. During the dry period the soil temperature presented a behavior similar to the wet one, but without the 10 cm minimum, and presenting smoother signals; also, cold fronts left a well delineated signature, specially in the soil temperature series, with strong gradients which may affect the microorganisms in the soil.

Concerning the soil thermal properties, no values were found in the literature for soils covered by dense forests, although, as well highlighted by Sharratt (1997), in studies for others types of forests, the future assessments of heat and water exchange within forests should consider near surface properties of the forest floors. The variations of heat capacity (C) during the dry period at the pasture were consistent with the values quoted by Verhoef et al. (1996) for a reddish sandy loam soil of a vineyard in Spain and a loamy soil of a savanna in Niger. The computed apparent soil thermal diffusivities (α) for the pasture confirmed the results obtained by Alvalá et al. (1996) for the both period, and are consistent with the values given by Verhoef et al. (1996) for soil moisture content less than 0.15 $m^3 m^{-3}$ at a savanna. However, they are higher than the

values for wet sand given by Rosenberg et al. (1983) and Arya (1988). The computed apparent soil conductivity ($\lambda = C\alpha$) values were consistent with the ones measured by Verhoef et al. (1996) for the above mentioned sites, except at pasture during the wet season, whose maximum value of λ appeared surprisingly high (around 5 W m^{-1} K^{-1}), compared with largest values of λ for sand recorded under wet conditions by Riha et al. (1980), with $\theta = 0.38$ m^3 m^{-3}.

These results showed that differences in flux, temperature and soil thermal properties can be explained in terms of different variations in moisture content and different soil-surface energy balances of the two vegetation types. Also, indicate that further studies, including measurements of the soil thermal properties, should be made at both sites, as well as in other Amazonian soil types.

Acknowledgements

This work is part of the LBA and was supported by FAPESP (Fundação de Amparo à Pesquisa do Estado de São Paulo) - grant 1997/9926-9. Thanks are due to J. L. Esteves (INCRA/Ji-Paraná) and C. Brandão (IBAMA/Ji-Paraná) and their staffs, for support during the field campaign. To A. I. Harada and S. B. M. Sambatti for data processing. R. C. S. Alvalá, A. O. Manzi and H. R. Rocha are supported by research fellowships funded by CNPq/Brazil (Conselho Nacional de Desenvolvimento Científico e Tecnológico).

References

Alvalá, R. C. S., R. Gielow, I. R. Wright, and M. G. Hodnett, Thermal diffusivity of Amazonian soils, in *Amazonian Deforestation and Climate*, edited by J. H. Gash, C. A. Nobre, J. M. Roberts, R. L. Vitoria, R. L, pp. 139-150, John Wiley, New York, 1996.

Arya, S. P. (Ed.) , *Introduction to micrometeorology*., 307 pp. Academic Press, New York, 1988.

Braud, I., A. C. Dantas-Antonino, M. Vauclin, J. L. Thony, and P. Ruelle, A simple soil plant atmosphere transfer model (SiSPAT): development and field verification, *J. Hydrol*., *166*, 213-250, 1994.

Campbell, G. S. (Ed.), *Soil physics with basic. Transport models for soil-plant systems*. 1st ed., 155 pp. Elsevier Science Publishers, New York, 1985.

de Vries, D. A., Thermal properties of soils, in *Physics of plant environment*, 2nd ed., edited by W. R. van Wijk, pp. 210-235, North Holland Publishing Company, Amsterdam, 1966.

Hodnett, M. G., M. D. Oyama, and J. Tomasella, Comparisons of long-term soil water storage behaviour under pasture and forest in three areas of Amazonia, in *Amazonian Deforestation and Climate*, edited by J. H. Gash, C. A. Nobre, J. M. Roberts, R. L. Vitoria, R. L, pp. 57-77, John Wiley, New York, 1996.

Horton, P., P. J. Wierenga, and D. R. Nielsen, Evaluation of methods for determining the apparent thermal diffusivity of soil near the surface, *Soil Sci. Soc. Am. J*., *47*, 25-32, 1983.

INPE, Boletim de monitoramento e análise climática, *Climanálise, 14, No. 08*, 1999.

Lettau, H. H., Improved models of thermal diffusion in the soil, *Trans. Am. Geophys. Union*, *35,* 121-132, 1954.

McWilliam, A. -L. C., O. M. R. Cabral, B. M. Gomes, J. L. Esteves, and J. R. Roberts, Forest and pasture leaf gas exchange in south-west Amazonia, in *Amazonian Deforestation and Climate*, edited by J. H. Gash, C. A. Nobre, J. M. Roberts, R. L. Vitoria, R. L, pp. 265-285, John Wiley, New York, 1996.

Nassar, J. N., and R. Horton, Determination of the apparent thermal diffusivity of a nonuniform soil. *Soil Sci, 147*(4), 238-244, 1989.

Novak, M. D., and T. A. Black, Theoretical determination of the surface energy balance and thermal regimes of bare soils, *Boundary-Layer Meteor*., *33*, 313-333, 1985.

Passerat de Silans, A. M. B., B. A. Monteny, and J. P. Lhomme, Apparent soil thermal diffusivity, a case study: HAPEX-Sahel experiment. *Agric. For. Meteor*., *81*, 201-216, 1996.

Passerat de Silans, A. M. B., L. Bruckler, J. L. Thony, and M. Vauclin, Numerical modeling of coupled heat and water flows during drying in a startified bare soil. Comparison with field observations, *J. Hydrol*., *105*, 109-138, 1989.

Ralston, A., and H. S. Wilf (Eds.), *Mathematical methods for digital computers*. John Wiley & Sons, New York, 1964.

Riha, S. J., K. J. McInnes, S. W. Clids, and G. S. Campbell, A finite element calculation for determining thermal conductivity, *Soil Sci. Soc. Am. J., 44*, 1323-1325.

Rosenberg, N. J., B. L. Blad, and S. B. Vertma (Eds.), *Microclimate: the biological environment*. John Wiley & Sons, New York, 1983.

Sharratt, B. S., Thermal conductivity and water retention of a black spruce forest floor, *Soil Science, 162*, 576-582.

Smirnova, T. G., J. M. Brown, and S. G. Benjamin, Performance of different soil model configuration in simulating ground surface temperature and surface fluxes, *Mon. Wea. Rev*., *125*, 1870-1884, 1997.

Smith, C. B. M. N. Lakhtakia, W. J. Capehart, and T. N. Carlson, Initialization of soil-water content for regional-scale atmospheric prediction models. *Bull. Amer. Meteor. Soc., 75*, 585-593, 1994.

van Wijk, W. R., and W. J. Derksen, Sinusoidal temperature variation in a layered soil, in *Physics of Plant Environment,* 2nd ed, edited by van Wijk, W. R., pp. 171-206, North Holland Publishing Company, Amsterdam, 1966.

Verhoef, A., B. J. J. M. van den Hurk, A. F. G. Jacobs, and B. G. Heusinkveld, Thermal soil properties for vineyard (EFEDA-I) and savanna (HAPEX-Sahel) sites, *Agric. For. Meteor.*, *78*, 1-18, 1996.

Figure Legends

Figure 1. Daily variation of air temperature, relative humidity, soil heat flux, soil volumetric water content, soil temperature and rainfall measured at forest - February 1999.

Figure 2. Same as Fig. 1 at pasture - February 1999.

Figure 3. Same as Fig. 1 at forest - August 1999

Figure 4. Same as Fig. 1 at pasture - August 1999

Figure 5. Temperature extrema for the DOY 225 cold front.

Figure 6. Soil moisture content and rainfall at forest - September 1999.

Figure 7. Same as Fig. 6 at pasture - September 1999.

Figure 8. Soil moisture content at 20 cm depth versus soil storage in the 10-40 cm layer.

Figure 9. Daily apparent soil thermal properties at forest - February 1999.

Figure 10. Same as Fig. 9 at pasture - February 1999.

Figure 11. Same as Fig. 9 at forest - August 1999.

Figure 12. Same as Fig. 9 at pasture - August 1999.

Figure 13. Computed apparent soil thermal diffusivities versus soil moisture content in the 10 - 40 cm layer.

Figure 14. Soil temperatures measured and calculated at 20 cm depth at forest (DOYS 43, 56, 227, 237) and at pasture (DOYS 38, 56, 225, 238).

Table 1. Forest and Pasture Soil Densities and Porosities.

Soil sample depth cm	Forest		Pasture	
	Dry bulk density (ρ) Kg/m^3	Porosity %	Dry bulk density (ρ) Kg/m^3	Porosity %
0 - 5	1,160	56.0	1,400	47.0
7.50 - 12.50	1,500	43.4	1,570	40.8
17.50 - 22.50	1,550	41.5	1,580	40.4
37.50 - 42.50	1,560	41.1	1,430	46.0

Table 2. Gravimetric vs FDR Soil Moisture Contents.

Site	Depth (cm)	DOY-LST	θ (Gravimetric) $m^3\ m^{-3}$	θ (FDR) $m^3\ m^{-3}$	FDR/Gravimetric
	10	32 - 12:20	0.23	0.23	1.00
Forest	20	32 - 12:10	0.22	0.26	1.18
	40	32 - 16:00	0.26	0.30	1.15
	10	54 - 15:25	0.23	0.20	0.87
Pasture	20	54 - 15:25	0.25	0.21	0.84
	40	54 - 17:40	0.22	0.22	1.00
					***Average* 1.01**

Table 3. Monthly Statistics of Sampled Measured Energy Components, Atmospheric and Soil Data at Forest and Pasture During the Wet Period.

	$K\downarrow$ ($W\ m^{-2}$)	T_{air} (C)	RH (%)	G ($W\ m^{-2}$)	T_{10cm} (C)	T_{20cm} (C)	T_{40cm} (C)	θ_{10cm} $m^3\ m^{-3}$	θ_{20cm} $m^3\ m^{-3}$	θ_{40cm} $m^3\ m^{-3}$	Rainfall (mm/30')
					Forest - February 1999						
Average	-	25.05*	88.4*	-2.04	24.78	24.93	25.01	0.198	0.205	0.219	-
STD	-	2.32	11.5	11.65	0.37	0.27	0.18	0.029	0.031	0.020	-
Max	n.a.	32.3	100	177.10	25.85	25.68	25.46	0.372	0.357	0.286	21.3
Min		21.4	52	-58.36	24.04	24.33	24.68	0.151	0.158	0.189	0
					Pasture - February 1999						
Average	-	24.83*	89.9*	0.41	26.59	26.93	26.49	0.242	0.270	0.312	-
STD	-	2.47	11.3	34.29	1.49	1.04	0.66	0.038	0.022	0.020	-
Max	1194.6	31.45	100	167.1	31.09	29.72	27.94	0.331	0.335	0.398	16.72
Min	0	20.85	43.2	-147.17	23.67	24.48	24.84	0.159	0.220	0.280	0

STD - standard deviation, n.a. - not available, * - incomplete series (see Figures 1a,b; 2a,b).

Table 4. Monthly Statistics of Sampled Measured Energy Components, Atmospheric and Soil Data at Forest and Pasture During the Dry Period.

	$K\downarrow$ (W m^{-2})	T_{air} (C)	RH (%)	G (W m^{-2})	T_{10cm} (C)	T_{20cm} (C)	T_{40cm} (C)	θ_{10cm} m^3 m^{-3}	θ_{20cm} m^3 m^{-3}	θ_{40cm} m^3 m^{-3}	Rainfall (mm/30')
					Forest - August 1999						
Average	-	25.94*	72.7*	-0.34	23.21	22.93	23.23	0.070	0.080	0.102	-
STD	-	4.43	19.3	9.73	1.55	1.15	0.80	0.003	0.010	0.004	-
Max	887.18	33.63	100	26.05	26.06	24.83	24.50	0.088	0.137	0.126	9.68
Min	0	14.34	32	-44.35	18.61	19.67	21.19	0.067	0.075	0.099	0
					Pasture - August 1999						
Average	-	24.54	61.2*	7.87	24.14	24.70	24.54	0.058	0.091	0.125	-
STD	-	5.52	18.6	50.17	2.68	1.88	1.23	0.046	0.044	0.029	-
Max	887.7	34.36	95.2	134.47	29.53	28.21	26.80	0.258	0.230	0.213	24.68
Min	0	11.13	30.1	-134.20	16.60	19.23	21.20	0.037	0.074	0.112	0

STD standard deviation, n.a. - not available, * - incomplete series (see Figures 3a,b; 4b)

Table 5. Monthly Statistics of Measured Daily Accumulated Energy Fluxes at Forest and Pasture During the Wet Period.

	$K\downarrow$ (MJ m^{-2})	a	R_n (MJ m^{-2})	G (MJ m^{-2})	$R_n/K\downarrow$	G/R_n
			Forest - February 1999			
Average	16.80	n.a.	12.63	-0.18	0.715	-0.015
STD	4.75	n.a.	3.53	0.16	0.082	0.014
Max	24.41	n.a.	21.79	0.20	1.035	0.011
Min	6.45	n.a.	6.69	-0.52	0.645	-0.049
			Pasture - February 1999			
Average	17.37	0.20*	11.27	0.04	0.650	-0.008
STD	3.71	0.003	2.42	0.37	0.037	0.039
Max	24.04	0.20	15.37	0.99	0.732	0.046
Min	8.54	0.19	5.70	-0.76	0.596	-0.111

STD - standard deviation, a = albedo, n.a. = not available, * = incomplete series

Table 6. Monthly Statistics of Measured Daily Accumulated Energy Fluxes at Forest and Pasture During the Dry Period.

	$K\downarrow$ (MJ m^{-2})	a	R_n (MJ m^{-2})	G (MJ m^{-2})	$R_n/K\downarrow$	G/R_n
			Forest - August 1999			
Average	18.84	0.15*	11.01	-0.03	0.583	-0.001
STD	2.06	0.01	1.67	0.31	0.043	0.028
Max	21.65	0.17	14.99	0.28	0.711	0.026
Min	15.25	0.14	8.20	-1.12	0.509	-0.097
			Pasture - August 1999			
Average	17.83	0.24	7.74	0.72	0.435	0.091
STD	3.71	0.01	0.97	0.37	0.045	0.140
Max	20.59	0.26	9.53	1.69	0.542	0.182
Min	13.42	0.21	5.78	-2.89	0.359	-0.412

STD - standard deviation, a = albedo, * incomplete series

Table 7. Monthly Statistics of Daily Soil Thermal Properties at Forest and Pasture During the Wet and Dry Period.

	$\theta_{10\text{-}40cm}$ ($m^3\ m^{-3}$)	C ($MJm^{-3}K^{-1}$)	$\alpha \times 10^6$ (m^2s^{-1})	λ ($W\ m^{-1}\ K^{-1}$)	$\theta_{10\text{-}40cm}$ ($m^3\ m^{-3}$)	C ($MJm^{-3}K^{-1}$)	$\alpha \times 10^6$ (m^2s^{-1})	λ ($W\ m^{-1}\ K^{-1}$)
	Forest - February 1999				**Pasture - February 1999**			
Average	0.208	2.11	1.08	2.28	0.279	2.40	1.34	3.20
STD	0.024	0.10	0.44	0.98	0.020	0.09	0.37	0.90
Max	0.261	2.33	2.50	5.37	0.315	2.55	2.12	5.13
Min	0.171	1.95	0.27	0.63	0.233	2.20	0.50	1.17
	Forest - August 1999				**Pasture - August 1999**			
Average	0.086	1.60	0.55	0.85	0.097	1.64	1.16	1.91
STD	0.007	0.03	0.33	0.54	0.040	0.17	0.14	0.33
Max	0.120	1.74	1.49	2.37	0.219	2.14	1.69	2.85
Min	0.082	1.58	0.10	0.00	0.081	1.57	0.83	1.31

STD - standard deviation

Table 8. Bias and RMS Statistics Between Measured and Predicted Soil Temperatures at the 20 cm Depths of the 10-40 cm Layer.

	Forest - Wet		Pasture - Wet		Forest - Dry		Pasture - Dry	
	Bias	**RMS**	**Bias**	**RMS**	**Bias**	**RMS**	**Bias**	**RMS**
Average	0.03	0.08	0.30	0.33	-0.21	0.24	0.17	0.20
STD	0.08	0.06	0.04	0.03	0.07	0.07	0.03	0.03
Max	0.27	0.27	0.37	0.40	0.01	0.36	0.25	0.26
Min	-0.05	0.02	0.17	0.25	-0.34	0.05	0.09	0.11

STD - standard deviation

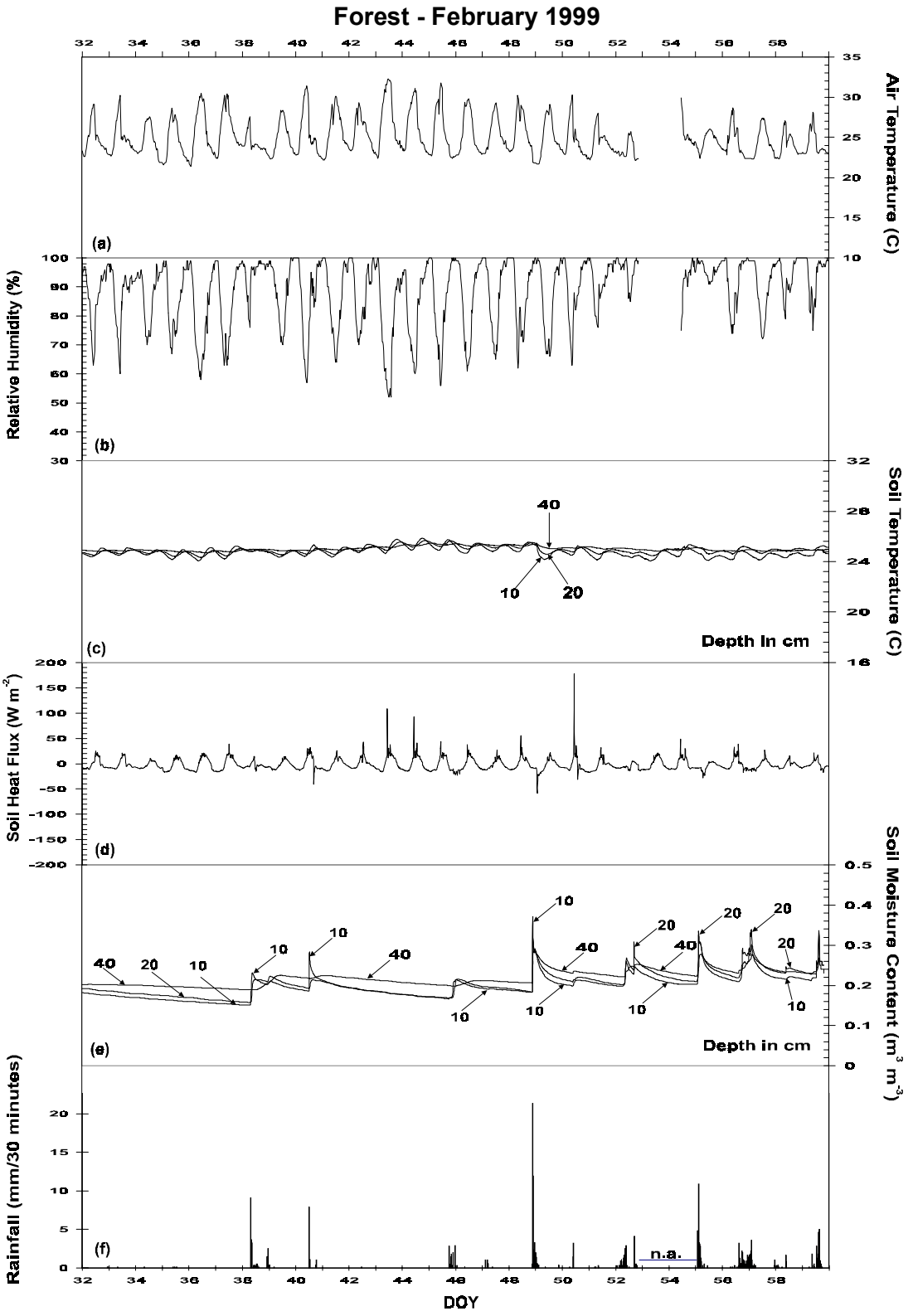

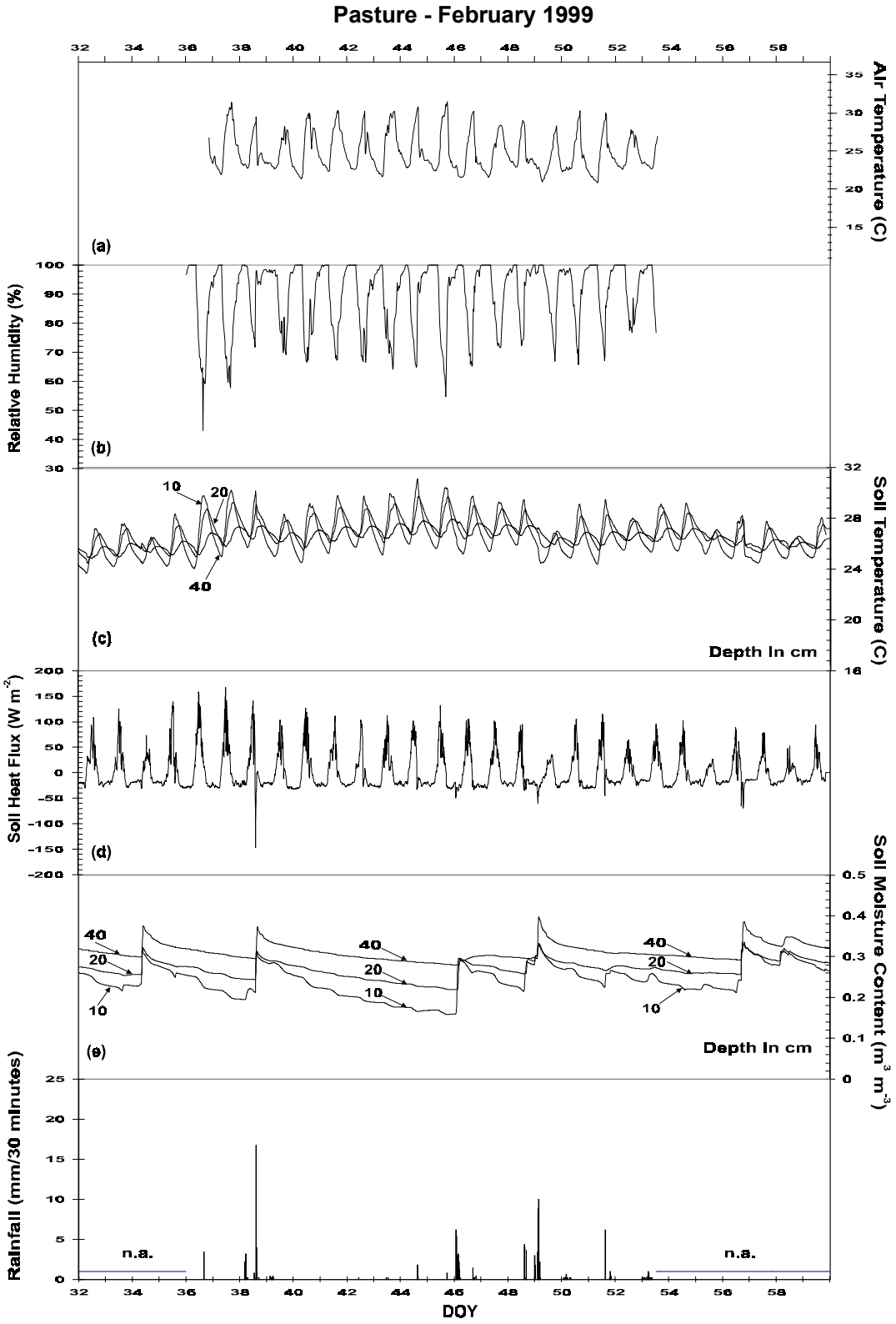

Figure 2

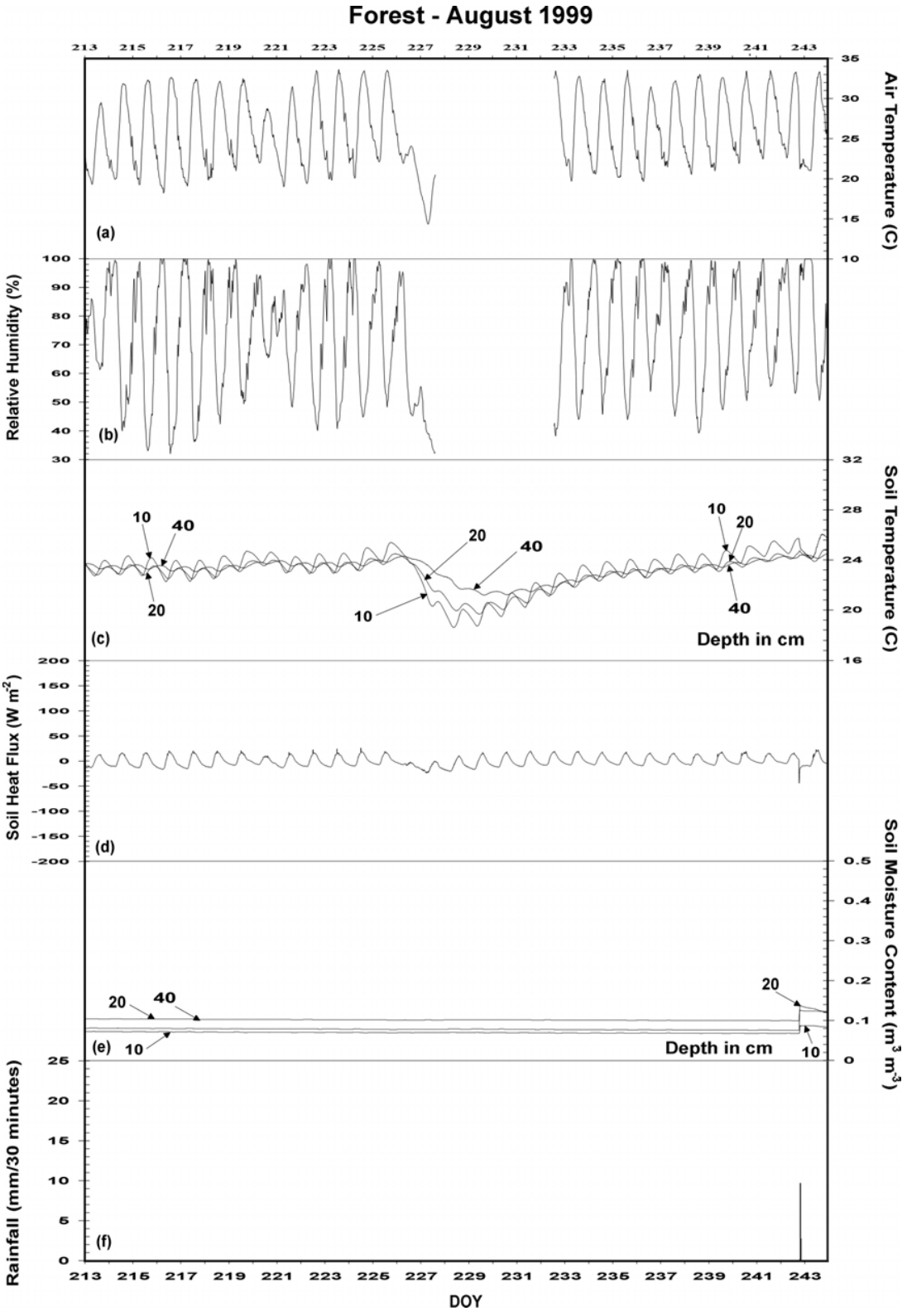

Figure 3

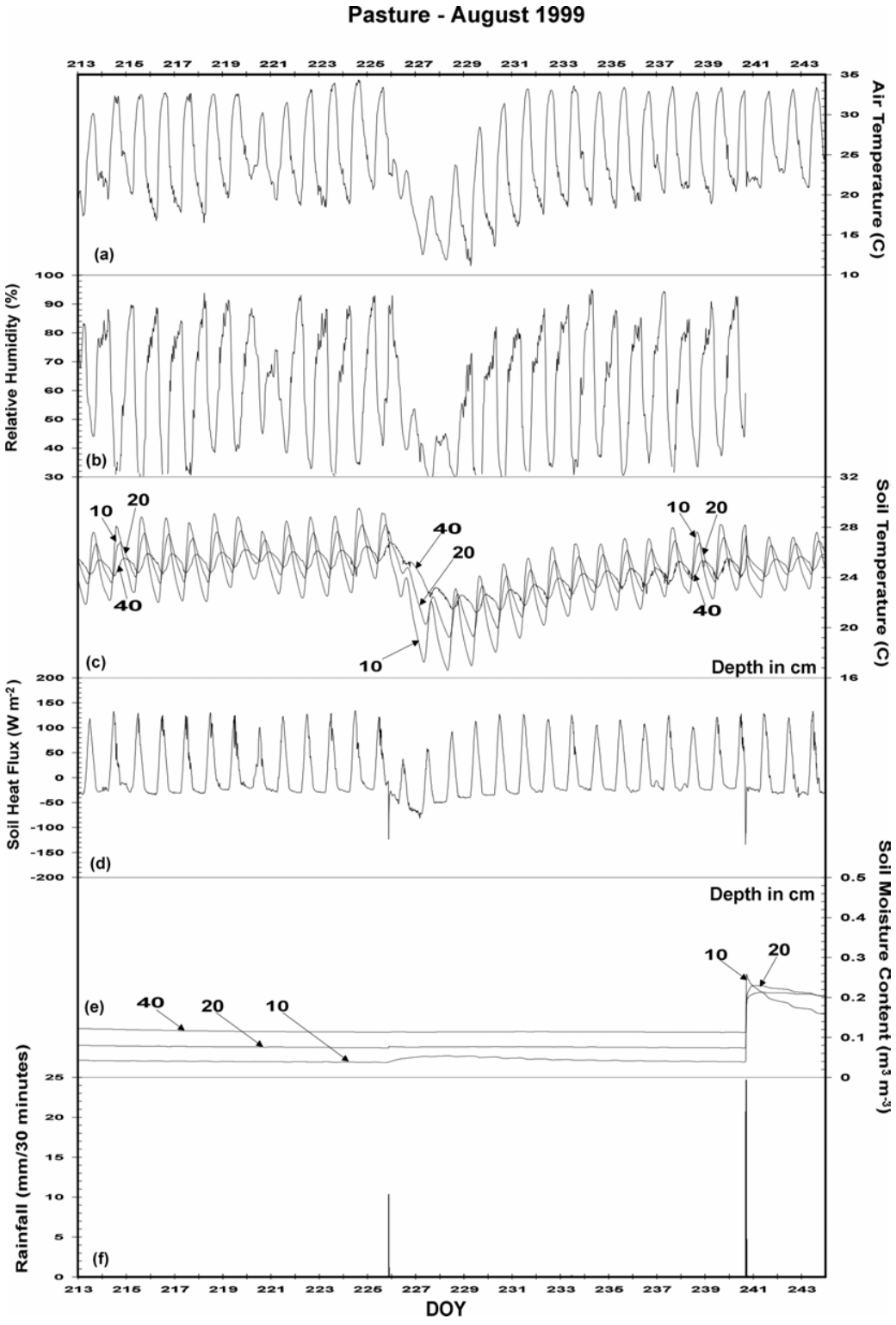

Figure 4

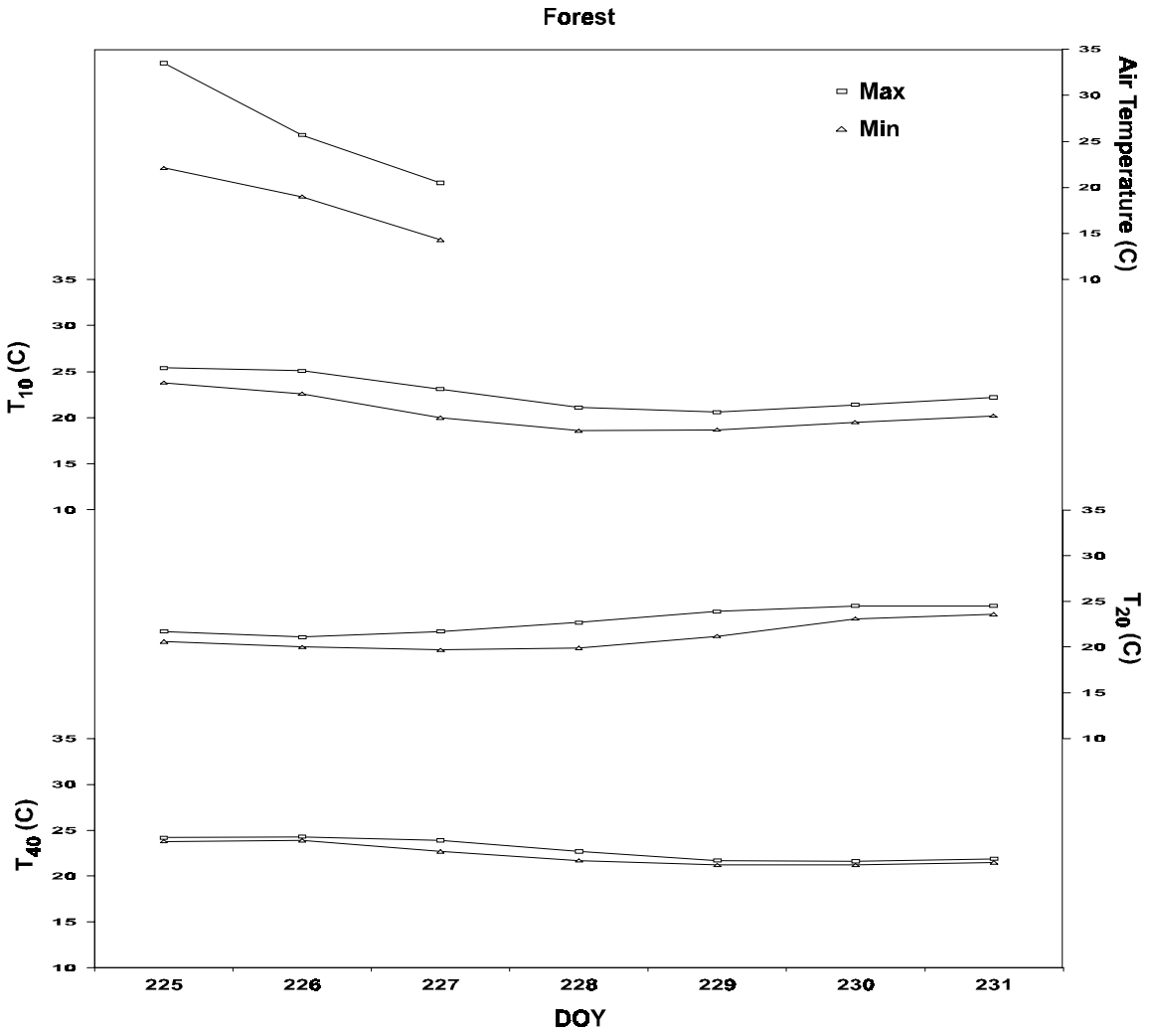

Figure 5a

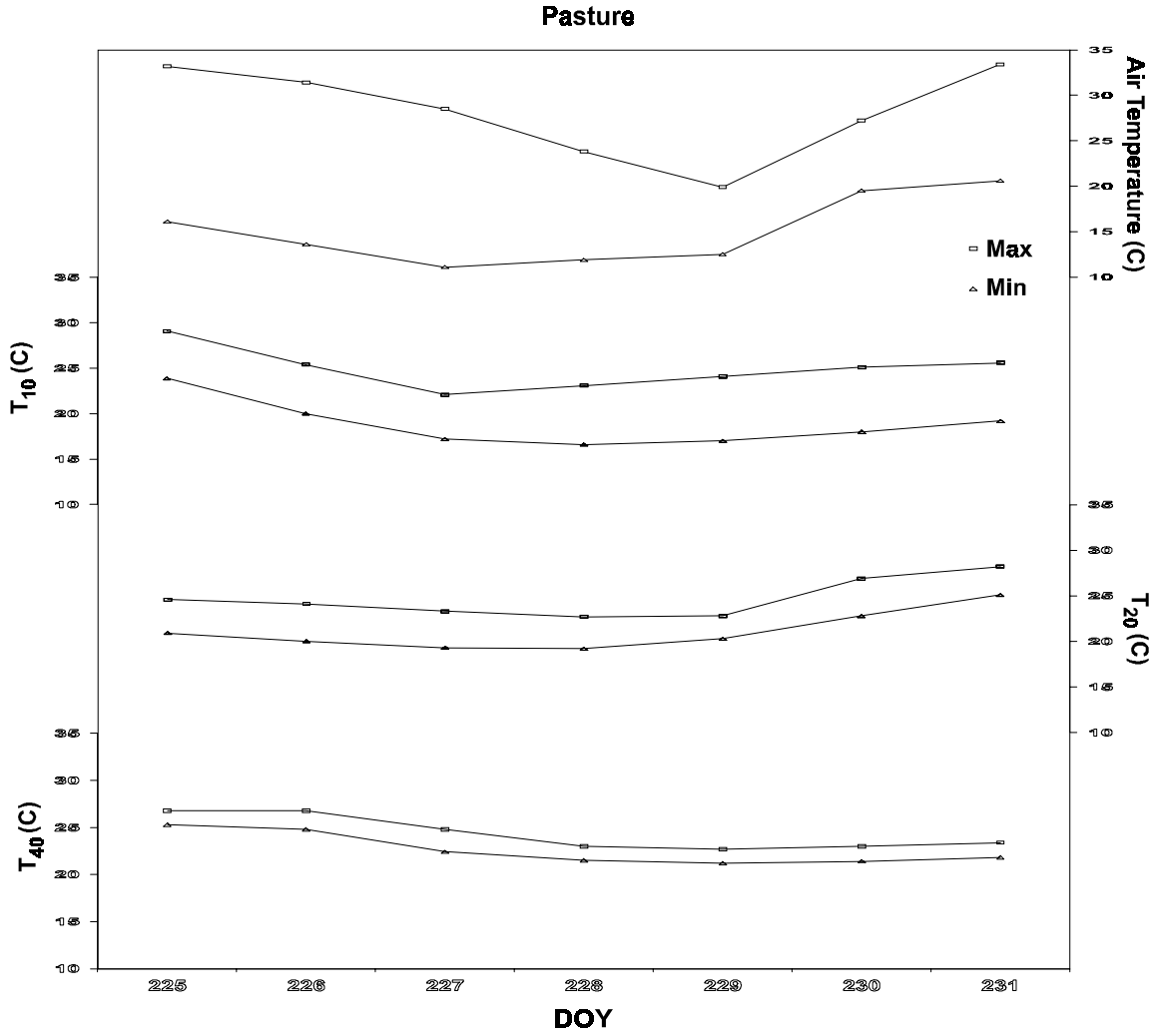

Figure 5b

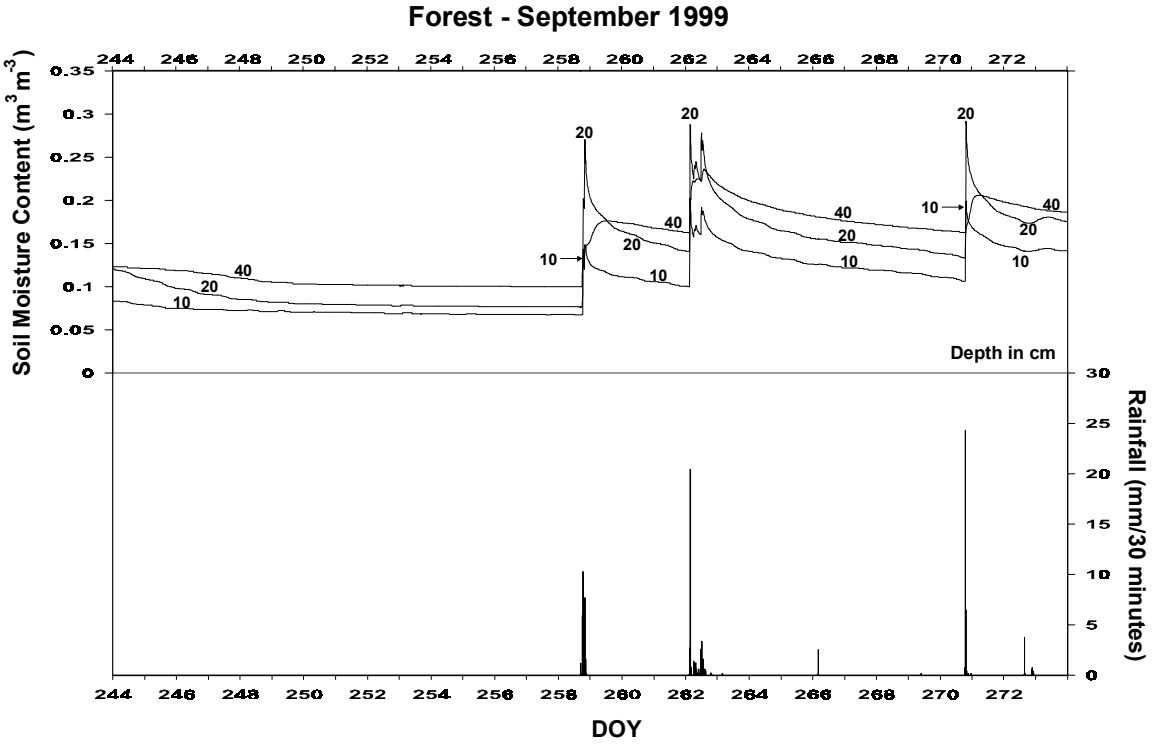

Figure 6

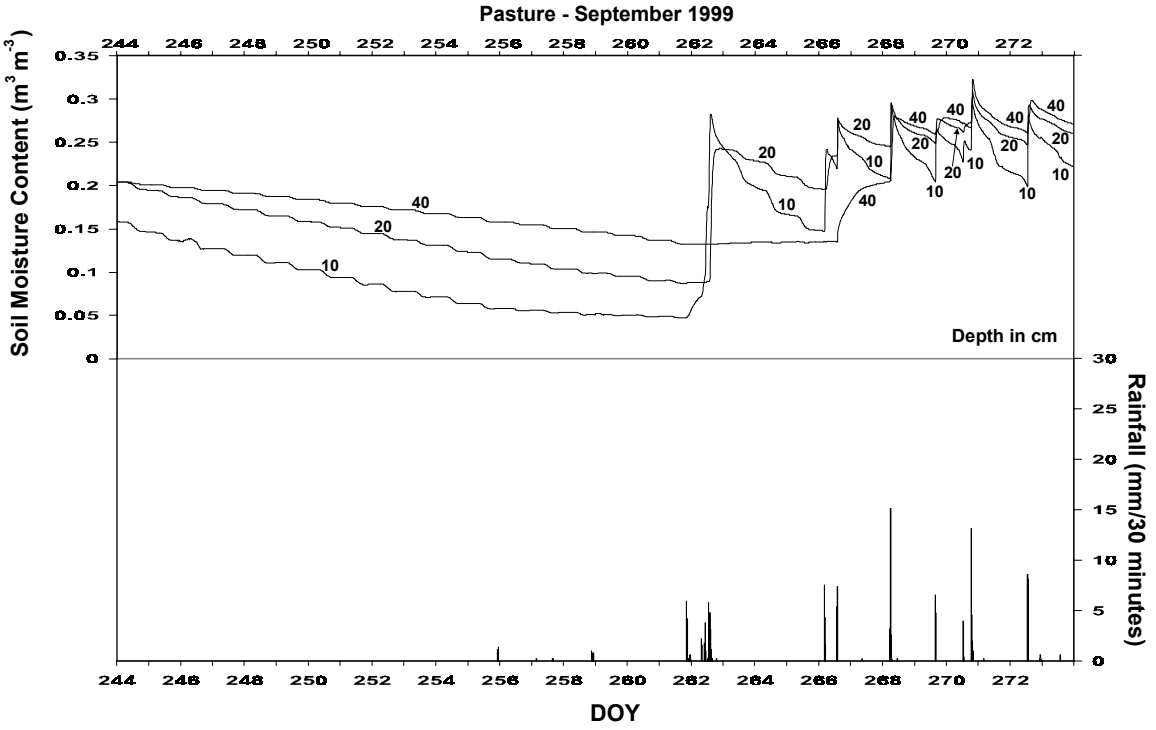

Figure 7

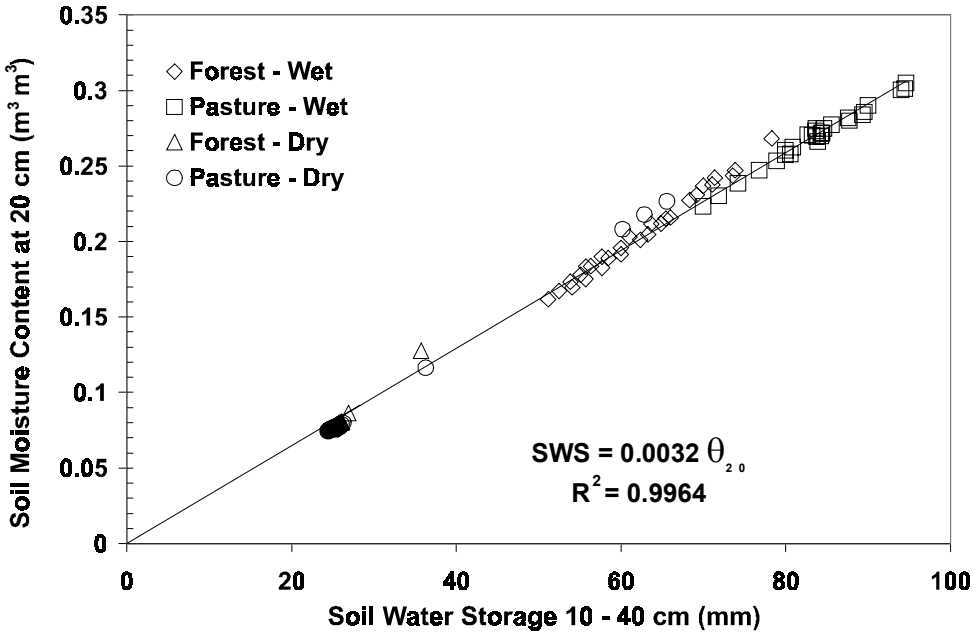

Figure 8

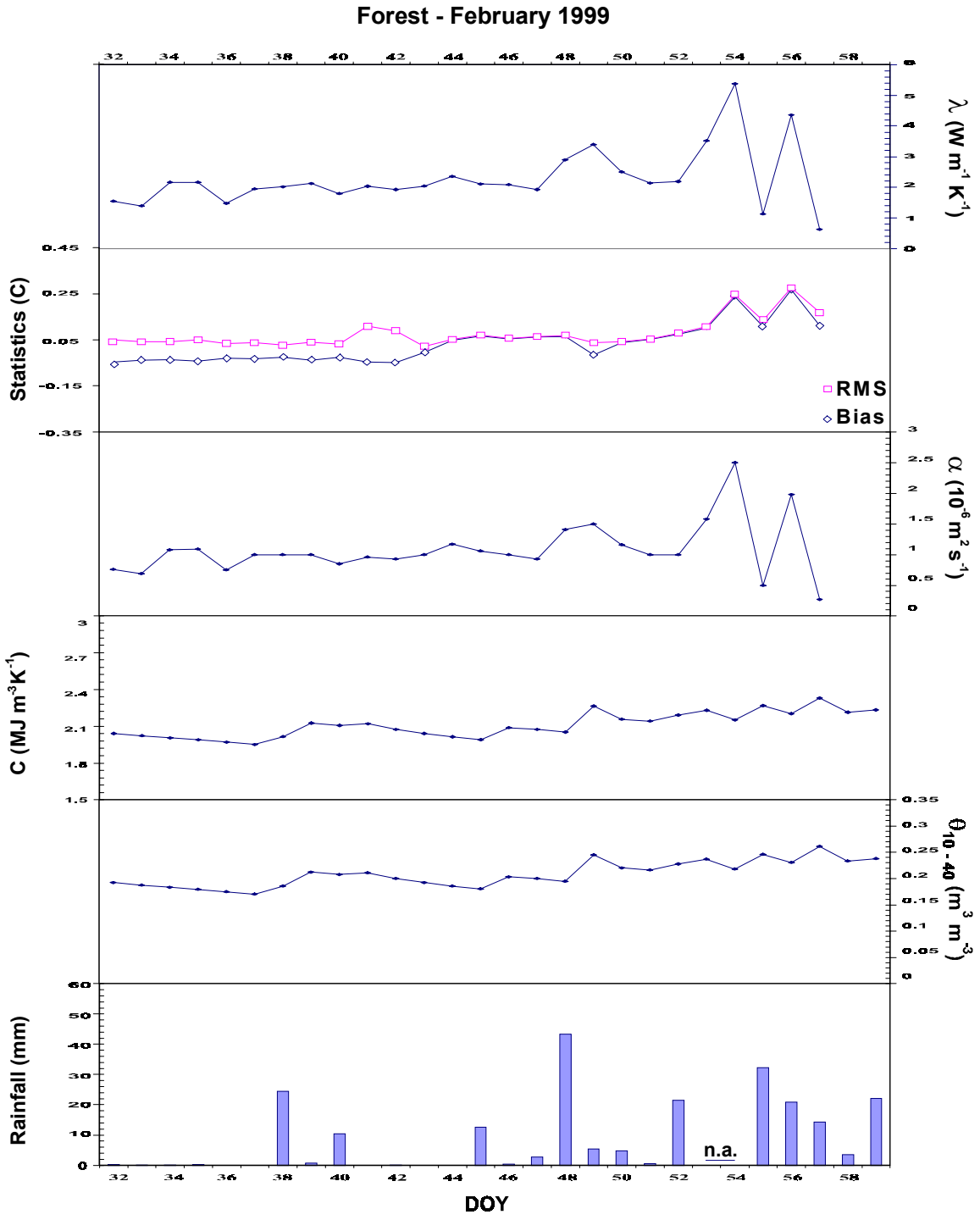

Figure 9

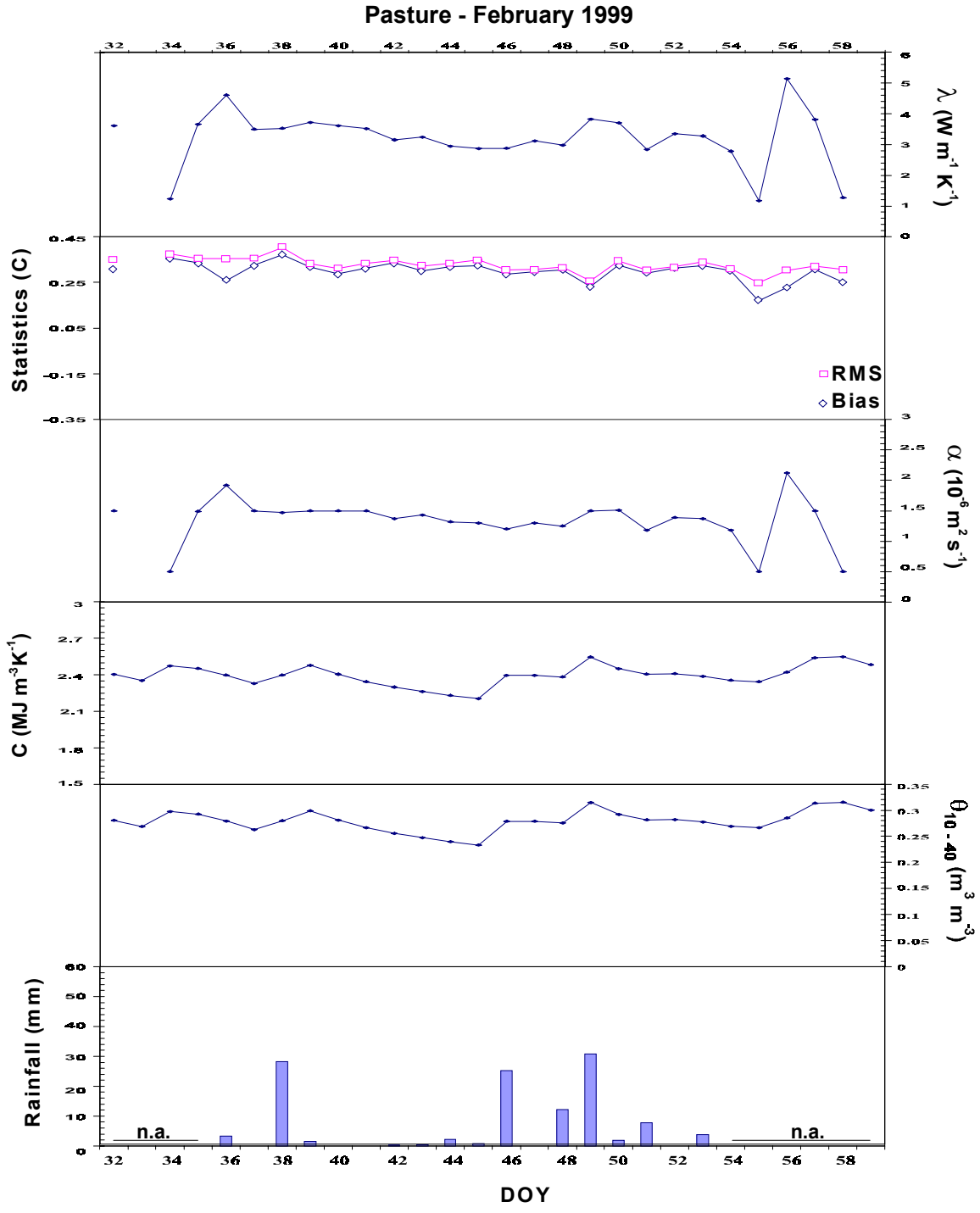
Pasture - February 1999
λ (W m-1 K-1)
Statistics (C)
RMS
Bias
α (10-6 m2 s-1)
C (MJ m-3K-1)
θ10 - 40 (m3 m-3)
Rainfall (mm)
n.a.
n.a.
DOY

Figure 10

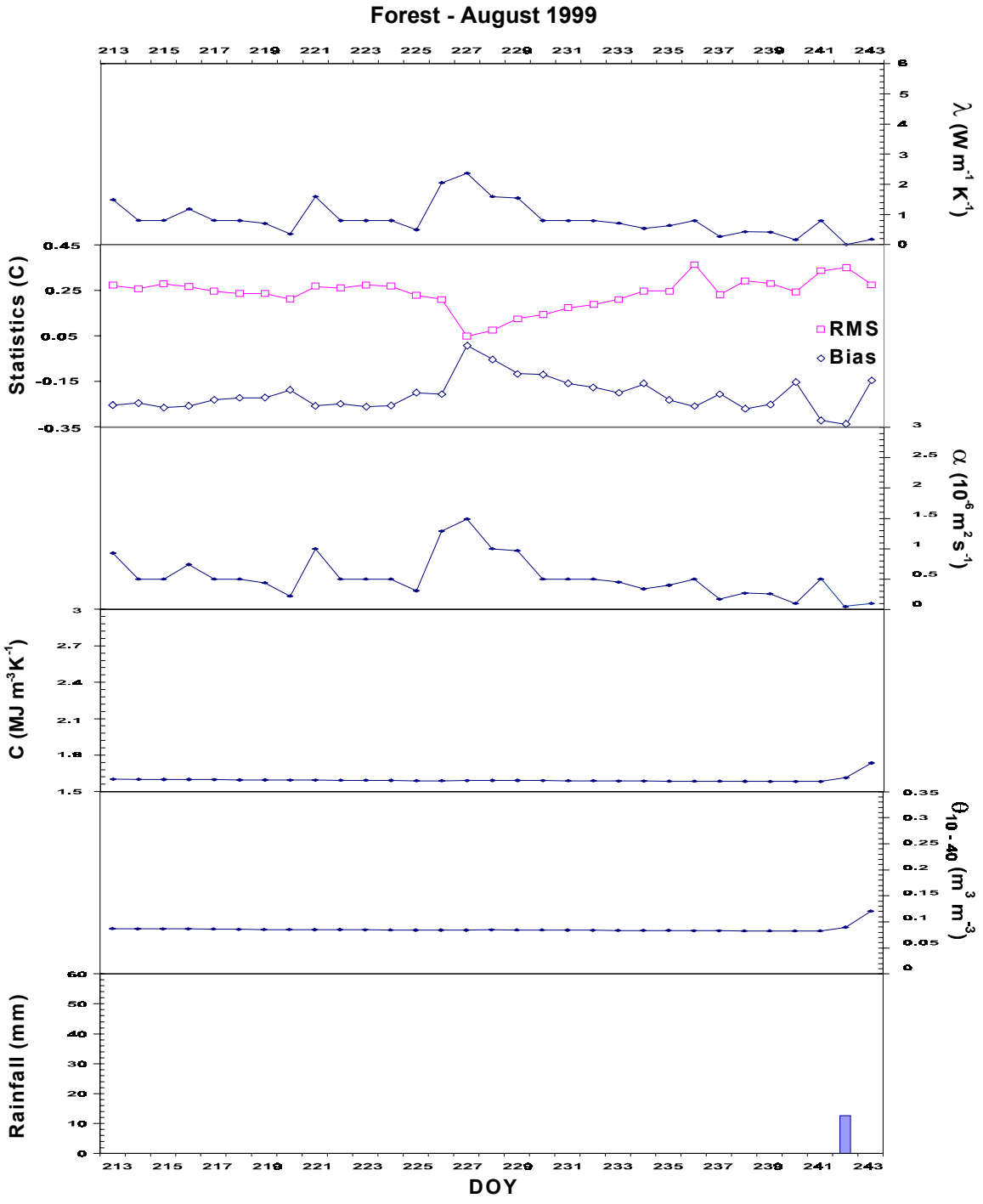

Figure 11

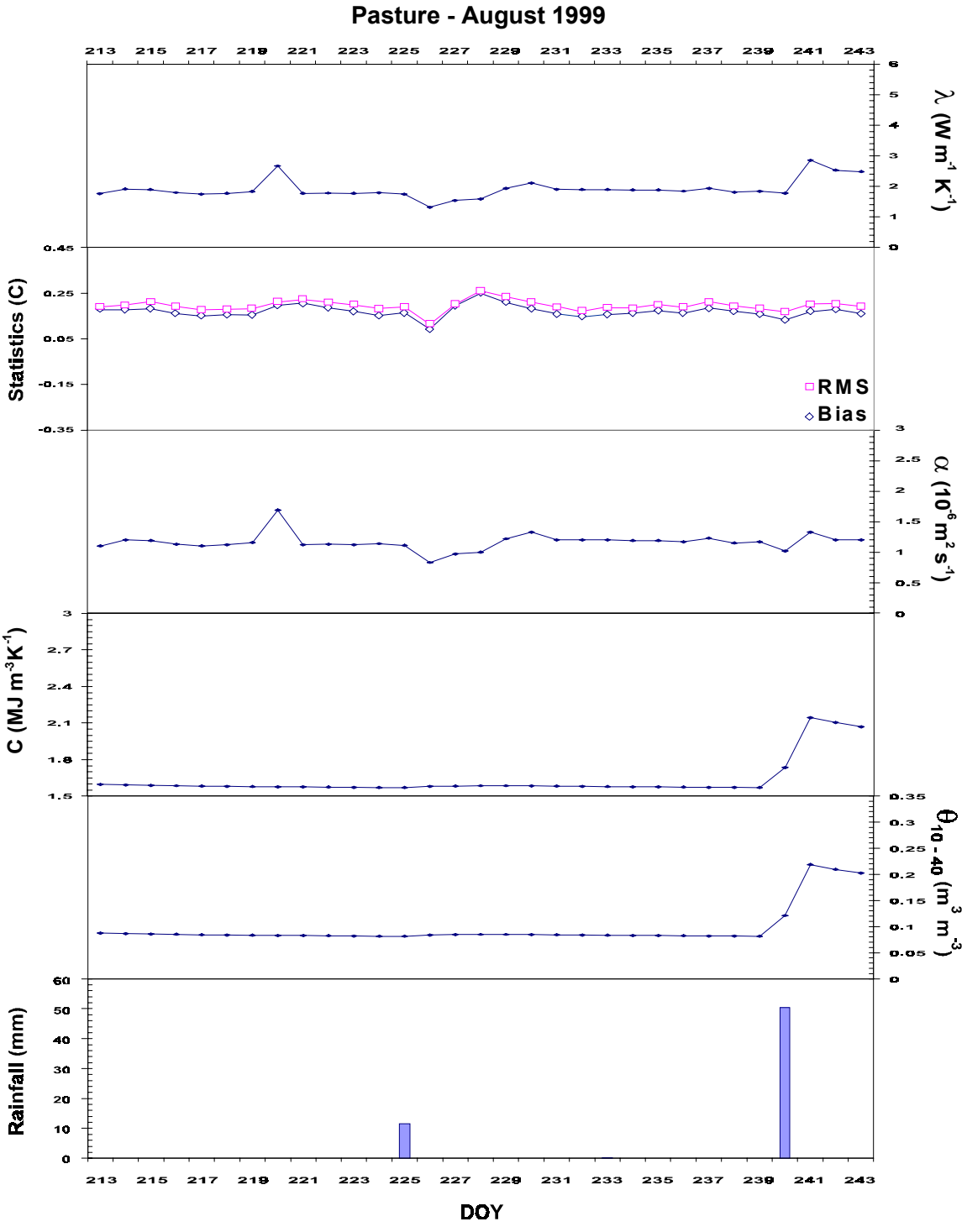

Figure 12

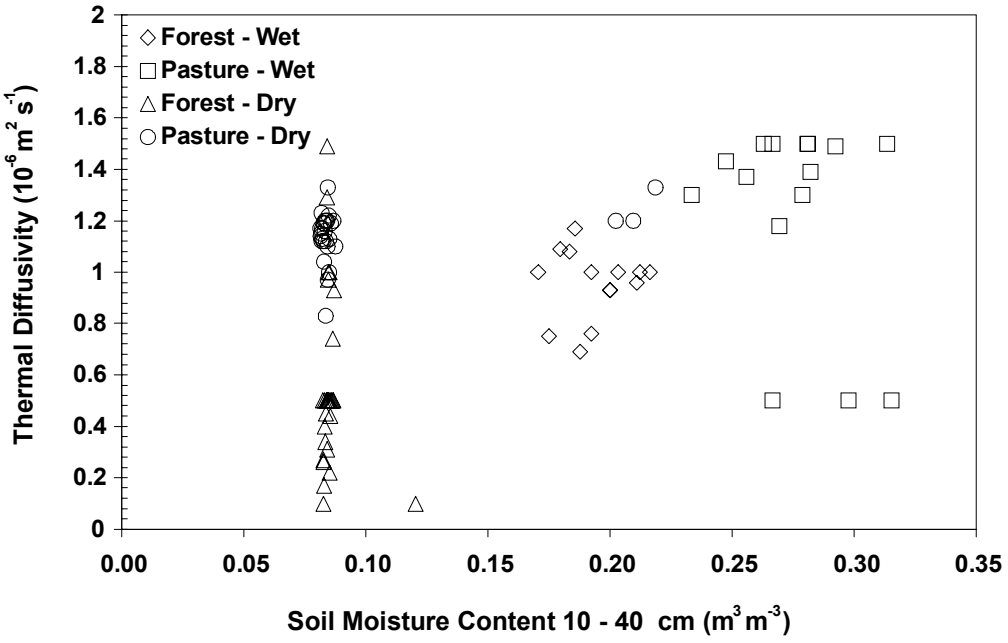

Figure 13

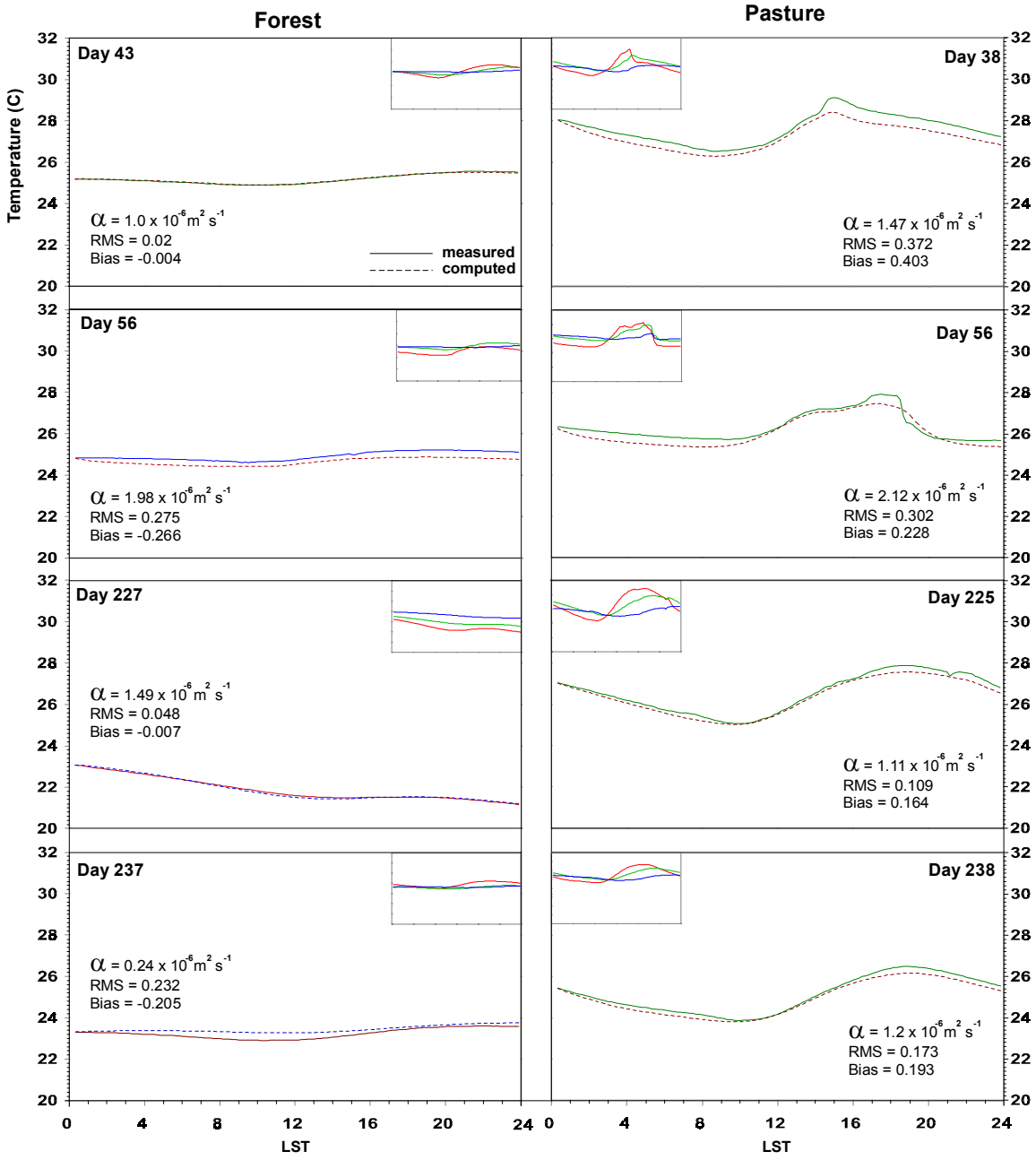
Forest
Pasture
Temperature (C)
Day 43
α = 1.0 x 10-6 m2 s-1
RMS = 0.02
Bias = -0.004
measured
computed
Day 38
α = 1.47 x 10-6 m2 s-1
RMS = 0.372
Bias = 0.403
Day 56
α = 1.98 x 10-6 m2 s-1
RMS = 0.275
Bias = -0.266
Day 56
α = 2.12 x 10-6 m2 s-1
RMS = 0.302
Bias = 0.228
Day 227
α = 1.49 x 10-6 m2 s-1
RMS = 0.048
Bias = -0.007
Day 225
α = 1.11 x 10-6 m2 s-1
RMS = 0.109
Bias = 0.164
Day 237
α = 0.24 x 10-6 m2 s-1
RMS = 0.232
Bias = -0.205
Day 238
α = 1.2 x 10-6 m2 s-1
RMS = 0.173
Bias = 0.193
LST
LST

Figure 14